PERGAMON

International Journal of Heat and Mass Transfer 44 (2001) 3823–3832

International Journal of HEAT and MASS TRANSFER

www.elsevier.com/locate/ijhmt

An algorithm for solving multidimensional inverse heat conduction problem

Somchart Chantasiriwan *

Faculty of Engineering, Thammasat University, Khlong Luang, Pathum Thani 12121, Thailand

Received 18 February 2000; received in revised form 7 January 2001

Abstract

The unknown time-dependent boundary heat flux of a multidimensional body is determined from temperature measurements inside the body or on its boundary. The sequential function specification method with the assumption that future-boundary heat flux varies linearly with time is used to solve the inverse problem. The method of discretization used by the proposed algorithm is the boundary element method. The effectiveness of the algorithm is illustrated by solving a sample two-dimensional problem. © 2001 Published by Elsevier Science Ltd.

1. Introduction

In a linear inverse heat conduction problem (IHCP), the unknown boundary heat flux of a solid body, of which thermophysical properties are known, is to be determined from temperature measurements inside the body or on the surface of the body. A number of solution techniques have been proposed for the one-dimensional IHCP [1–5]. The multidimensional IHCP, however, has received considerably less attention so far [6–8] despite the fact that most practical problems cannot be approximated as one-dimensional problems.

Among the methods proposed for multidimensional IHCP, the sequential function specification method appears to have the promise to be able to deal with IHCP efficiently. The method was first introduced by Beck et al. [1] for dealing with one-dimensional problems. The distinct feature of this method is its use of future-time temperature measurements to stabilize the estimation of the current heat flux component. This method requires the determination of sensitivity coefficients, defined as the temperature response at sensor locations to unit applied heat flux at the boundary where the heat flux is to be estimated. Later, Osman et al. [6] applied this method to two-dimensional problems. Whereas the determination of sensitivity coefficients for the one-dimensional IHCP is relatively easy because the analytical solution to the corresponding direct problem is known, the determination of sensitivity coefficients for the two-dimensional IHCP must be done using a numerical method. The finite element method is attractive for this purpose because of its ability to handle arbitrary geometry. Furthermore, the sensitivity coefficients could be determined using the existing finite-element codes.

Apart from the finite element method, another numerical method that is able to handle arbitrary geometry is the boundary element method. For problems having no source term, the boundary element enjoys an important advantage over the finite-element method in that no domain mesh generation is required. The boundary element method was previously used to solve the steady-state IHCP [9,10] and the one-dimensional time-dependent IHCP [2]. In this paper, multidimensional time-dependent IHCP will be considered. The solution will be stabilized by the sequential function specification method with the piecewise linear basis function and the assumption of linearly varying boundary heat flux components. Recent results by Chantasiriwan [11] showed that this method yielded better estimates of boundary condition than the well-known sequential function specification method that uses the piecewise constant basis function and the assumption of constant boundary heat flux components [1]. However, the method previously presented can be applied to only one-dimensional problems. The generalization to multidimensional problems will be shown here. The following

* Tel.: +66-2-5646304; fax: +66-2-5646303.
E-mail address: somchart@engr.tu.ac.th (S. Chantasiriwan).

0017-9310/01/$ - see front matter © 2001 Published by Elsevier Science Ltd.
PII: S0017-9310(01)00037-0

Nomenclature

A	$M_n \times M_n$ diagonal matrix
a	coefficient that depends on $\vec{\xi}$
B	$r(M_1 + M_2) \times M_3$ matrix
$\vec{C}$	vector of temperature measurements
D	$M_3 \times r(M_1 + M_2)$ matrix
$E(y)$	expected value of random variable y
f	interior temperature
G	fundamental solution
g	known boundary heat flux
H_n	transformation matrix
i, j, k	dummy indices
L	the number of nodes in an element
M_1	the number of sensors on Γ_1
M_2	the number of sensors inside the object
M_3	the number of heat flux components on Γ_2 which are to be determined
M_c	the number of additional heat flux components at corner or edge nodes
M_e	the number of boundary elements
M_n	the number of boundary nodes
m	dimension of the problem
N	number of time intervals
n	number of heat flux components to be estimated
$\vec{n}$	outward pointing unit vector normal to boundary
P_1	$M_n \times M_n$ matrix
P_2	$M_2 \times M_n$ matrix
R_1	$M_n \times M_3$ matrix
R_2	$M_2 \times M_3$ matrix
S_1	$M_n \times (M_n - M_3)$ matrix
S_2	$M_2 \times (M_n - M_3)$ matrix
q	boundary heat flux into the domain
r	future-time parameter
$\vec{r}$	position vector
T	temperature
t	time
U	analytical solution to a heat conduction problem
X	$(M_1 + M_2) \times M_3$ matrix
X_1	$M_n \times M_3$ matrix
X_2	$M_2 \times M_3$ matrix
x	position of sensor
$\vec{Y}$	vector of temperature measurements
$\vec{Z}$	vector of unknown heat flux components
$V(y)$	variance of random variable y

Greek symbols

Δ	deterministic bias
ε	temperature measurement error
Φ	interpolating function
ϕ	function relating boundary temperature to boundary temperature
Γ	boundary
Γ_1	part of the boundary where heat flux is known
Γ_2	part of the boundary where heat flux is to be determined
σ^2	variance in temperature measurement
τ	time
ψ	function relating boundary temperature to boundary heat flux
$\vec{\xi}$	position vector

Subscripts

i, j, k, l, m	boundary element indices, boundary node indices, space indices or matrix element indices

Superscripts

i, j, k, N	time indices

sections will describe the statement of the problem, the discretization of the problem using the boundary element method, the proposed sequential function specification algorithm, and the results and discussion of the application of this algorithm to the sample problem. Finally, the conclusion will follow.

2. Statement of the problem

Consider a solid object with part of its boundary Γ_1 subjected to known heat flux $g(\vec{r}, t)$ and the remaining part of the boundary Γ_2 subjected to unknown heat flux $Z(\vec{r}, t)$. Suppose that the object has constant thermophysical properties, making the problem a linear one. Without the loss of generality, we can take the value of the thermal diffusivity to be unity and the initial condition to be homogeneous. The heat conduction process can therefore be described by the following equations:

$$\frac{\partial T(\vec{r}, t)}{\partial t} = \nabla^2 T(\vec{r}, t), \tag{1}$$

$$T(\vec{r}, 0) = 0, \tag{2}$$

$$\vec{n}\vec{\nabla} T(\vec{r}, t) = g(\vec{r}, t) \quad \text{for } \vec{r} \text{ on } \Gamma_1. \tag{3}$$

Let temperature sensor be located at $\vec{r}_i$, and let measurements be taken at time $j\Delta t$.

$$T(\vec{r}_i, j\Delta t) = Y_i^{(j)}. \tag{4}$$

The temperature sensors may be located on the boundary or inside the object. If the unknown boundary heat flux Z is assumed to be a piecewise linear function of

position and time, Eqs. (1)–(4) can be solved for heat flux components at selected boundary nodes.

3. Formulation of the boundary element method

In this section, the formulation of the boundary element method for subsequent application to the IHCP will be derived. The boundary element formulation for a time-dependent linear heat conduction problem is given by [12]

$$aT(\vec{\xi},t)=\int_\Gamma\int_0^t q(\vec{r},\tau)G(\vec{r}-\vec{\xi};t-\tau)\,\mathrm{d}\tau\,\mathrm{d}\vec{r}-\int_\Gamma\int_0^t T(\vec{r},\tau)\vec{n}\vec{\nabla}G(\vec{r}-\vec{\xi};t-\tau)\,\mathrm{d}\tau\,\mathrm{d}\vec{r},\quad(5)$$

where q is heat flux, a is coefficient that depends on $\vec{\xi}$, and the fundamental solution G is

$$G(\vec{r}-\vec{\xi};t-\tau)=\frac{\mathrm{e}^{-(\vec{r}-\vec{\xi})^2/4(t-\tau)}}{[4\pi(t-\tau)]^{m/2}}\quad(6)$$

and m is 2 for two-dimensional problem or 3 for three-dimensional problem. Divide the boundary Γ into M_e boundary elements and time t into N equal time intervals. Eq. (5) becomes

$$aT(\vec{\xi},t)=\sum_{i=1}^{M_e}\int_{\Gamma_i}\left[\sum_{j=1}^{N}\int_{(j-1)\Delta t}^{j\Delta t}{}_iq(\vec{r},\tau)G(\vec{r}-\vec{\xi};N\Delta t-\tau)\,\mathrm{d}\tau\right]\mathrm{d}\vec{r}-\sum_{i=1}^{M_e}\int_{\Gamma_i}\left[\sum_{j=1}^{N}\int_{(j-1)\Delta t}^{j\Delta t}{}_iT(\vec{r},\tau)\vec{n}\vec{\nabla}G(\vec{r}-\vec{\xi};N\Delta t-\tau)\,\mathrm{d}\tau\right]\mathrm{d}\vec{r},\quad(7)$$

where the front subscript denotes element index. Next let us approximate ${}_iq$ and ${}_iT$ by piecewise linear functions in time:

$${}_iq(\vec{r},\tau)=\frac{1}{\Delta t}\left[{}_iq^{(j)}(\vec{r})-{}_iq^{(j-1)}(\vec{r})\right](\tau-N\Delta t)+{}_iq^{(j)}(\vec{r})(N-j+1)-{}_iq^{(j-1)}(\vec{r})(N-j),\quad(8)$$

$${}_iT(\vec{r},\tau)=\frac{1}{\Delta t}\left[{}_iT^{(j)}(\vec{r})-{}_iT^{(j-1)}(\vec{r})\right](\tau-N\Delta t)+{}_iT^{(j)}(\vec{r})(N-j+1)-{}_iT^{(j-1)}(\vec{r})(N-j),\quad(9)$$

where superscript denotes time index. Now approximate ${}_iq^{(j)}$ and ${}_iT^{(j)}$ over element i, making use of interpolating function Φ_k, as follows:

$${}_iq^{(j)}(\vec{r})=\sum_{k=1}^{L}{}_{i,k}q^{(j)}\Phi_k(\vec{r}),\quad(10)$$

$${}_iT^{(j)}(\vec{r})=\sum_{k=1}^{L}{}_{i,k}T^{(j)}\Phi_k(\vec{r}),\quad(11)$$

where k is local node index, and L is the number of nodes in an element. Each element is assumed to contain the equal number of local nodes. Substituting Eqs. (8)–(11) into Eq. (7) yields

$$\begin{aligned}aT(\vec{\xi},t)=&\sum_{i=1}^{M_e}\sum_{k=1}^{L}\left\{\int_{\Gamma_i}\left[\sum_{j=1}^{N}\int_{(j-1)\Delta t}^{j\Delta t}\left(\frac{(\tau-N\Delta t)}{\Delta t}+(N-j+1)\right)G\,\mathrm{d}\tau\right]\Phi_k(\vec{r})\,\mathrm{d}\vec{r}\right\}({}_{i,k}q^{(j)})\\&-\sum_{i=1}^{M_e}\sum_{k=1}^{L}\left\{\int_{\Gamma_i}\left[\sum_{j=1}^{N}\int_{(j-1)\Delta t}^{j\Delta t}\left(\frac{(\tau-N\Delta t)}{\Delta t}+(N-j)\right)G\,\mathrm{d}\tau\right]\Phi_k(\vec{r})\,\mathrm{d}\vec{r}\right\}({}_{i,k}q^{(j-1)})\\&-\sum_{i=1}^{M_e}\sum_{k=1}^{L}\left\{\int_{\Gamma_i}\left[\sum_{j=1}^{N}\int_{(j-1)\Delta t}^{j\Delta t}\left(\frac{(\tau-N\Delta t)}{\Delta t}+(N-j+1)\right)\vec{n}\vec{\nabla}G\,\mathrm{d}\tau\right]\Phi_k(\vec{r})\,\mathrm{d}\vec{r}\right\}({}_{i,k}T^{(j)})\\&+\sum_{i=1}^{M_e}\sum_{k=1}^{L}\left\{\int_{\Gamma_i}\left[\sum_{j=1}^{N}\int_{(j-1)\Delta t}^{j\Delta t}\left(\frac{(\tau-N\Delta t)}{\Delta t}+(N-j)\right)\vec{n}\vec{\nabla}G\,\mathrm{d}\tau\right]\Phi_k(\vec{r})\,\mathrm{d}\vec{r}\right\}({}_{i,k}T^{(j-1)}).\end{aligned}\quad(12)$$

If Eq. (12) is evaluated at a point $\vec{\xi}_k$ on the boundary or inside the object, the resulting equation after the assembly process can be written as

$$a_kT_k^{(N)}=\sum_{j=1}^{N}\sum_{i=1}^{M_n}\phi(\vec{\xi}_k,\vec{r}_i,(N-j)\Delta t)T_i^{(j)}+\sum_{j=1}^{N}\sum_{i=1}^{M_n+M_c}\psi(\vec{\xi}_k,\vec{r}_i,(N-j)\Delta t)q_i^{(j)},\quad(13)$$

where the back subscript denotes global node index, M_n is the number of boundary nodes, and M_c is the number of additional heat flux components at corner or edge nodes. Note that coefficient a_k becomes unity if $\vec{\xi}_k$ is inside the object. For two-dimensional problems, each corner node can have two heat flux components; therefore, M_c is equal to the number of corners. For three-dimensional problems, each edge node can have two heat flux components, and each corner node can have three heat flux components. Function ϕ, denoting function that relates boundary temperature to boundary temperature, and function ψ, denoting function that relates boundary temperature to boundary heat flux, are obtained from the evaluation of integrals shown in Eq. (12). The evaluation of time integrals can

be done exactly, whereas the evaluation of boundary integrals should be performed using the Gaussian quadrature.

Suppose that there are a total of $M_1 + M_2$ sensors, with M_1 sensors on the boundary and M_2 sensors inside the object. In addition, suppose that there are M_n nodes on the boundary, M_3 of which are locations of unknown heat flux components to be determined. Eq. (13) is now written for M_n boundary node points and M_2 interior sensor locations, yielding $M_n + M_2$ equations, which may be expressed as the two following matrix equations:

$$A\vec{T}^{(N)} = \sum_{j=1}^{N} P_1^{(N-j)}\vec{T}^{(j)} + \sum_{j=1}^{N} R_1^{(N-j)}\vec{Z}^{(j)} + \sum_{j=1}^{N} S_1^{(N-j)}\vec{g}^{(j)}, \tag{14}$$

$$\vec{f}^{(N)} = \sum_{j=1}^{N} P_2^{(N-j)}\vec{T}^{(j)} + \sum_{j=1}^{N} R_2^{(N-j)}\vec{Z}^{(j)} + \sum_{j=1}^{N} S_2^{(N-j)}\vec{g}^{(j)}, \tag{15}$$

where A is the $M_n \times M_n$ diagonal matrix of coefficients a; $\vec{T}^{(j)}$ is the vector of boundary temperatures at time $j\Delta t$; $\vec{f}^{(j)}$ is the vector of temperature measurements at interior sensor locations at time $j\Delta t$; $\vec{Z}^{(j)}$ is the vector of unknown heat flux components at time $j\Delta t$; $\vec{g}^{(j)}$ is the vector of known boundary heat flux components at time $j\Delta t$; $M_n \times M_n$ matrix $P_1^{(N-j)}$ and $M_2 \times M_n$ matrix $P_2^{(N-j)}$ are related to ψ; and $M_n \times M_3$ matrix $R_1^{(N-j)}$, $M_2 \times M_3$ matrix $R_2^{(N-j)}$, $M_n \times (M_n - M_3)$ matrix $S_1^{(N-j)}$, and $M_2 \times (M_n - M_3)$ matrix $S_2^{(N-j)}$ are related to ϕ.

Let $\vec{T}_0^{(j)}$ and $\vec{f}_0^{(j)}$ be, respectively, the boundary and interior temperature responses at time $j\Delta t$, which are the solution to the direct heat conduction problem described by Eqs. (1)–(3) and an additional boundary condition

$$\vec{n}\vec{\nabla}T(\vec{r},t) = 0 \quad \text{for } \vec{r} \text{ on } \Gamma_2. \tag{16}$$

$\vec{T}_0^{(N)}$ and $\vec{f}_0^{(N)}$ can then be written as

$$A\vec{T}_0^{(N)} = \sum_{j=1}^{N} P_1^{(N-j)}\vec{T}_0^{(j)} + \sum_{j=1}^{N} S_1^{(N-j)}\vec{g}^{(j)}, \tag{17}$$

$$\vec{f}_0^{(N)} = \sum_{j=1}^{N} P_2^{(N-j)}\vec{T}_0^{(j)} + \sum_{j=1}^{N} S_2^{(N-j)}\vec{g}^{(j)}. \tag{18}$$

If $\vec{g}$ is known as a function of time, $\vec{T}_0^{(N)}$ and $\vec{f}_0^{(N)}$ can be determined by a time-stepping procedure. Subtracting Eq. (17) from Eq. (14) and Eq. (18) from Eq. (15) results in

$$A\left[\vec{T}^{(N)} - \vec{T}_0^{(N)}\right] = \sum_{j=1}^{N} P_1^{(N-j)}\left[\vec{T}^{(j)} - \vec{T}_0^{(j)}\right] + \sum_{j=1}^{N} R_1^{(N-j)}\vec{Z}^{(j)}, \tag{19}$$

$$\left[\vec{f}^{(N)} - \vec{f}_0^{(N)}\right] = \sum_{j=1}^{N} P_2^{(N-j)}\left[\vec{f}^{(j)} - \vec{f}_0^{(j)}\right] + \sum_{j=1}^{N} R_2^{(N-j)}\vec{Z}^{(j)}. \tag{20}$$

Applying the time-stepping procedure to Eqs. (19) and (20) gives us the following relations between the boundary and interior temperatures and the unknown boundary heat flux:

$$\vec{T}^{(k)} - \vec{T}_0^{(k)} = \sum_{j=1}^{k} X_1^{(j-k)}\vec{Z}^{(k)}, \tag{21}$$

$$\vec{f}^{(k)} - \vec{f}_0^{(k)} = \sum_{j=1}^{k} X_2^{(j-k)}\vec{Z}^{(k)}, \tag{22}$$

where $X_1^{(j-k)}$ is $M_n \times M_3$ matrix, and $X_2^{(j-k)}$ is $M_2 \times M_3$ matrix. Of the M_n equations for boundary temperatures in the matrix equation (21), only M_1 equations, corresponding to M_1 boundary sensor locations, are to be used for the determination of the unknown boundary heat flux. These equations are combined with M_2 equations represented by the matrix equation (22). The result can be written as

$$\vec{Y}^{(k)} - \vec{Y}_0^{(k)} = \sum_{j=1}^{k} X^{(k-j)}\vec{Z}^{(j)}, \tag{23}$$

where $\vec{Y}^{(k)}$ is the vector of temperature measurements on the boundary and inside the object at time $k\Delta t$, $\vec{Y}_0^{(k)}$ is the vector temperatures at these sensor locations when $\vec{Z}^{(j)} = 0$ from $j = 1$ to k, and $X^{(k-j)}$ is $(M_1 + M_2) \times M_3$ matrix.

4. Sequential function specification method

The sequential function specification algorithm that makes use of piecewise linear functions for boundary heat flux and the assumption of linearly varying heat flux over future time was described by Chantasiriwan [11]. However, that algorithm is restricted to one-dimensional problems. The present paper will demonstrate that the algorithm can be extended to deal with multi-dimensional problems.

Suppose that $\vec{Z}^{(1)}$ to $\vec{Z}^{(k-1)}$ are known from earlier calculations of heat flux, and $\vec{Z}^{(k)}$ is to be determined in the next calculation. Eq. (8) can be rewritten as

$$\vec{Y}^{(i)} - \vec{Y}_0^{(i)} = \sum_{j=1}^{k-1} X^{(i-j)}\vec{Z}^{(j)} + \sum_{j=k}^{i} X^{(i-j)}\vec{Z}^{(j)}. \tag{24}$$

The sequential function specification method uses r future-temperature measurements $\vec{Y}^{(i)}$ (where i ranges from k to $k + r - 1$) to estimate $\vec{Z}^{(k)}$. Eq. (24) actually represents r matrix equations with r unknown vectors $(\vec{Z}^{(k+1)}, \vec{Z}^{(k+2)}, \ldots, \vec{Z}^{(k+r-1)})$. In order to reduce the

number of unknown vectors to one, the following relations between $\vec{Z}^{(j)}$ $(j = k, k+1, \ldots, k+r-1)$ and $\vec{Z}^{(k-1)}$, $\vec{Z}^{(k)}$ are specified:

$$\vec{Z}^{(j)} = (j-k+1)\vec{Z}^{(k)} - (j-k)\vec{Z}^{(k-1)}. \tag{25}$$

Substitute Eq. (25) into Eq. (24), and rearrange the result:

$$\vec{Y}^{(i)} - \vec{Y}_0^{(i)} = \sum_{j=1}^{k-1} X^{(i-j)}\vec{Z}^{(j)} - \vec{Z}^{(k-1)}\sum_{j=k}^{i}(j-k)X^{(i-j)} + \vec{Z}^{(k)}\sum_{j=k}^{i}(j-k+1)X^{(i-j)}. \tag{26}$$

Now define the following vector:

$$\vec{C}^{(k)} = \left[\vec{Y}^{(k)} \;\; \vec{Y}^{(k+1)} \;\; \ldots \;\; \vec{Y}^{(k+r-1)}\right]^{\mathrm{T}}, \tag{27}$$

which has $r(M_1+M_2)$ components. Also define the following $r(M_1+M_2)\times M_3$ matrices:

$$B^{(0)} = \left[X^{(0)} \;\; X^{(1)} + 2X^{(0)} \;\; \ldots \;\; \sum_{i=0}^{r-1}(i+1)X^{(r-i-1)}\right]^{\mathrm{T}}, \tag{28}$$

$$B^{(1)} = \left[X^{(1)} \;\; X^{(2)} - X^{(0)} \;\; \ldots \;\; X^{(r)} - \sum_{i=0}^{r-1} iX^{(r-i-1)}\right]^{\mathrm{T}}, \tag{29}$$

and

$$B^{(j)} = \left[X^{(j)} \;\; X^{(j+1)} \;\; \ldots \;\; X^{(j+r-1)}\right]^{\mathrm{T}} \quad (j = 2, 3, \ldots, k-1). \tag{30}$$

The r matrix equations represented by Eq. (26) can be rewritten as

$$\vec{C}^{(k)} = \sum_{j=1}^{k} B^{(k-j)}\vec{Z}^{(j)}. \tag{31}$$

Following the procedure in [11], we then seek the expression of the heat flux in terms of temperature measurements:

$$\vec{Z}^{(k)} = \sum_{j=1}^{k} D^{(k-j)}\vec{C}^{(j)}. \tag{32}$$

$M_3 \times r(M_1+M_2)$ matrices $D^{(k)}$ can be expressed in terms of $B^{(j)}$ as follows:

$$B^{(0)}D^{(0)} = I, \tag{33}$$

where I is the $r(M_1+M_2)\times r(M_1+M_2)$ identity matrix

$$B^{(0)}D^{(k)} = -\sum_{j=1}^{k} B^{(j)}D^{(k-j)} \tag{34}$$

for $1 \leqslant k \leqslant N-1$. If the number of temperature sensors is greater than the number of unknown heat flux components, matrices $D^{(k)}$ and $B^{(j)}$ may be rectangular, and the linear least-squares method should be used to determine $D^{(k)}$. Subroutine DGELSS.F in the numerical package LAPACK (available at http://www.netlib.org/lapack) may be used for this purpose.

5. Assessing the quality of the solution

The quality of a solution to IHCP depends on its variance and deterministic bias. Variance measures the sensitivity of the solution to temperature measurement errors. In general, these are statistical errors. It is expedient to make the following statistical assumptions about them:

1. Additive errors: $Y_i^{(k)} = \bar{Y}_i^{(k)} + \varepsilon_i^{(k)}$.
2. Zero mean errors: $E(\varepsilon_i^{(k)}) = 0$.
3. Constant variance: $V(\varepsilon_i^{(k)}) = \sigma^2$.
4. Uncorrelated errors: $E(\varepsilon_i^{(k)}\varepsilon_j^{(l)}) = 0$ if $i \neq j$ or $k \neq l$.

The estimated heat flux component i at time $k\Delta t$ can be expressed in terms of temperature measurements as

$$Z_i^{(k)} = \sum_{l=1}^{k}\sum_{m=1}^{r}\sum_{j=1}^{M_1+M_2} D_{i,(m-1)(M_1+M_2)+j}^{(k-l)} Y_j^{(l+m-1)}. \tag{35}$$

The above assumptions, together with Eq. (35), yield the following expression for variance of $Z_i^{(k)}$:

$$V\left(Z_i^{(k)}\right) = \sigma^2 \sum_{l=0}^{k-1}\sum_{m=1}^{r}\sum_{j=1}^{M_1+M_2}\left(D_{i,(m-1)(M_1+M_2)+j}^{(l)}\right)^2. \tag{36}$$

It is evident from Eq. (36) that variance of each estimated heat flux component increases monotonically with time index. Hence, maximum variance for component i is $V(Z_i^{(N)})$.

When measurements are error-free, $Y_i^{(k)} = \bar{Y}_i^{(k)}$, the calculated heat flux should closely approximate the true heat flux. Deterministic bias Δ indicates how good the approximation is:

$$(\Delta_i)^2 = \frac{1}{N}\sum_{k=1}^{N}\left(Z_i^{(k)} - Z_{i,\mathrm{actual}}^{(k)}\right)^2, \tag{37}$$

where $Z_{i,\mathrm{actual}}^{(k)}$ is the actual heat flux component i at time $k\Delta t$. In general, variance and deterministic bias will vary from component to component. Let us denote the maximum $V(Z_i^{(N)})$ by $V_{\max}$ and the maximum Δ_i by $\Delta_{\max}$. The quality of the solution to IHCP can now be characterized by $V_{\max}$ and $\Delta_{\max}$. Normally, both low variance and low deterministic bias are desirable. Unfortunately, when the variance of the solution to IHCP is reduced, the deterministic bias will normally increase, and vice versa. A good method for solving IHCP, like the sequential function specification method, will allow the user to arrive at the optimal solution, which has the desired trade-off between variance and deterministic bias.

6. Sample problem

The sample problem is illustrated in Fig. 1. A square object of unit length is subjected to heat flux on sides AB and BC, and insulated on the other two sides. Temperature measurements are taken from 13 equally spaced sensors located at a distance of x from AB and BC. The algorithm described earlier will be used to determine heat flux components on AB and BC using the temperature measurement data. For the purpose of generating such data, the heat flux on AB and BC is specified as shown in Fig. 2, which yields the following temperature distribution:

$$T(x,y,t) = \begin{cases} U(x,y,t) \quad \text{for } t \leqslant 0.5, \\ U(x,y,t) - 2U(x,y,t-0.5) \\ \quad \text{for } 0.5 < t \leqslant 1.0, \\ U(x,y,t) - 2U(x,y,t-0.5) \\ \quad + U(x,y,t-1.0) \quad \text{for } t > 1.0, \end{cases} \tag{38}$$

where

$$U(x,y,t) = 1.5t^2 + t\left(0.5x^2 - x + y^2 - 2y + 1\right) - 4\sum_{j=1}^{\infty} \frac{1}{(j\pi)^4}\left(0.5\cos(j\pi x) + \cos(j\pi y)\right) \times \left(1 - \mathrm{e}^{-j^2\pi^2 t}\right). \tag{39}$$

Note that the above analytical solution for this two-dimensional problem is the superposition of two solutions to one-dimensional problems, which can be easily found [1].

Temperature measurement data at 13 sensor locations will be assumed to be given by $T(x,y,t)$. They will be used to estimate heat flux on AB and BC, which will then be compared with the actual heat flux (Fig. 2) to assess the accuracy of the solution. For computational purpose, the boundary is divided into 48 equal elements. This problem is simplified by the fact that $\vec{g} = 0$. Hence, $\vec{Y}_0$ vanishes. The time step used for estimating the heat flux components is 0.05, and the calculation is performed from time 0 to 1.0. Hence, $N = 20$.

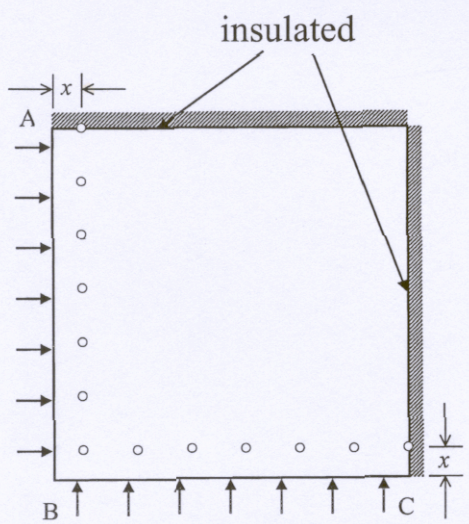

Fig. 1. Sample problem. The square object has the unit length. Unknown heat flux is applied to sides AB and BC. The other two sides are perfectly insulated. White circles represent temperature sensors.

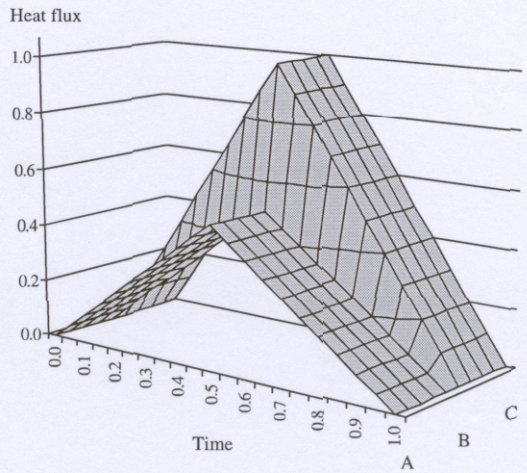

Fig. 2. Actual heat flux in the sample problem.

Although there are 13 nodes on AB and 13 nodes on BC, the number of unknown heat flux components to be determined will have to be less than 26. This is so because there are only 13 sensors. It has previously been suggested that the number of estimated heat flux components should be less than the number of sensors [1]. The proposed algorithm was tested with the case in which there were more estimated heat flux components than sensors, and it was found that no stabilized solution existed. Therefore, the number of nodes where heat flux components will be estimated from the proposed algorithm will have to be less than 13, and heat flux components at the remaining nodes can be found by linear interpolation of the estimated heat flux components. For this sample problem, let $\vec{Z}'^{(k)}_{\mathrm{AB}}$ denote the vector of n unknown heat flux components on AB to be determined from the inverse algorithm ($n < 13$), while $\vec{Z}^{(k)}_{\mathrm{AB}}$ denotes the vector of heat flux components at the 13 nodes on AB. In order for the unknown heat flux components to be equally spaced, n is limited to 7, 5, 4, 3, and 2. The relation between $\vec{Z}^{(k)}_{\mathrm{AB}}$ and $\vec{Z}'^{(k)}_{\mathrm{AB}}$ is

$$\vec{Z}^{(k)}_{\mathrm{AB}} = H_{\mathrm{n}}\vec{Z}'^{(k)}_{\mathrm{AB}}, \tag{40}$$

where the components of the $13 \times n$ matrix H_{n} are

$$(H_{\mathrm{n}})_{i,j} = \left[k + \frac{(n-1)(1-i)}{12}\right](2(k-j)+1) + j - k \tag{41}$$

for $1 \leqslant k \leqslant n-1$, $j = k$ or $k+1$, and

$$\frac{12(k-1)}{n-1} + 1 \leqslant i \leqslant \frac{12k}{n-1} + 1.$$

Other components are zero.

7. Results and discussion

First, let us consider the case in which the 13 sensors are placed at $x = 1/6$ from sides AB and BC, on which 10 heat flux components are to be determined. The resulting heat flux components are plotted in Fig. 3 for $r = 1$. It can be seen that though the actual heat flux is constant in space, there is a variation among the estimated heat flux components. Such a variation will increase rapidly as sensors are placed farther from AB. The regularization method, as used by Al-Khalidy [7], can suppress it. In this paper, an alternative method will be used. If the number of sensors is kept constant at 13, the estimated heat flux will become smoother as the number of heat flux components decrease from 10. Fig. 4 illustrates how the number of unknown heat flux components along AB and BC may be reduced.

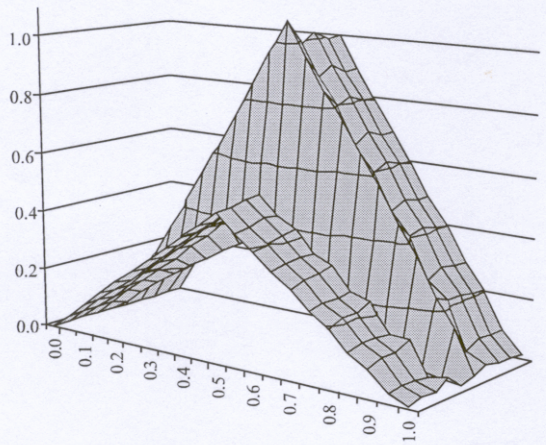

Fig. 3. Estimated heat flux for $n = 10$, $r = 1$, and $x = 1/6$.

Comparison between the solutions to the sample problem with 10 and 6 estimated heat flux components is shown in Fig. 5, in which composite curves of variations of heat flux components as functions of time are plotted. Fig. 5(a) is simply the view of the plot of Fig. 3 in the direction parallel to line ABC. It is evident that, with lower n, there is less variation among heat flux components. However, it should be kept in mind that restricting the number of estimated heat flux components may yield an inaccurate solution if the actual heat flux fluctuates in space with high frequency. In any case, the solution will be less sensitive to temperature measurement errors if there are fewer heat flux components to estimate.

Another way to reduce sensitivity to temperature measurement errors is to make use of 'future-time' measurements. The results shown in Fig. 5 are obtained by using future-time parameter $r = 1$. This means that no measurements taken later than $(k+1)\Delta t$ are used to estimate unknown heat flux components at time $k\Delta t$. By allowing r to be greater than 1, the variance of the solution will be reduced. Fig. 6 compares results for four cases having different r. Indicated on each figure are the values of maximum variance and maximum deterministic bias for each case. It can be seen that the solution is less sensitive to measurement errors as r is increased. However, by using more future-time measurements (or increasing r), the solution becomes less accurate not only in time but also in space as there is greater difference among the estimated heat flux components.

Another important factor that affects the variance and deterministic bias of the solution is the locations of

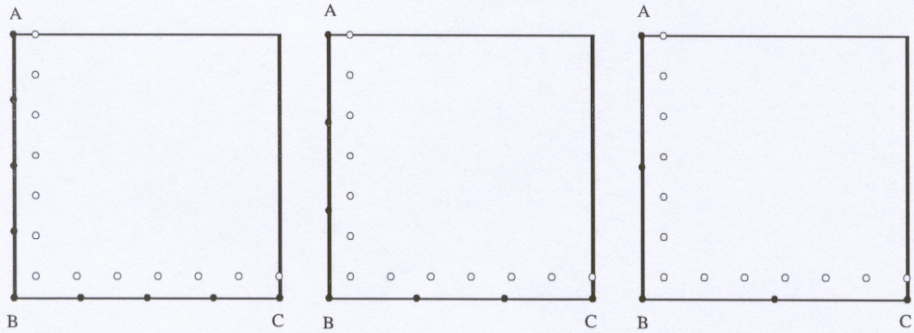

Fig. 4. Reducing the number of estimated heat flux components while keeping the number of sensors at 13. Solid circles denote locations of unknown heat flux components to be estimated from the inverse algorithm. Heat flux components at other boundary nodes may be determined from interpolation. Note that though one node is shown at point B, there are actually two heat flux components at that corner.

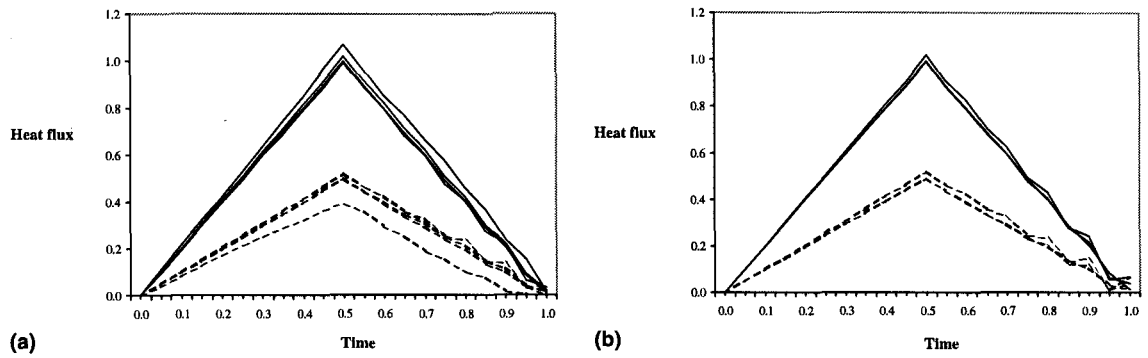

Fig. 5. Composite curves of variations of heat flux components as functions of time for (a) $n = 10$, (b) $n = 6$, $x = 1/6$, and $r = 1$. Dashed curves and solid curves represent, respectively, heat flux distribution along AB and BC.

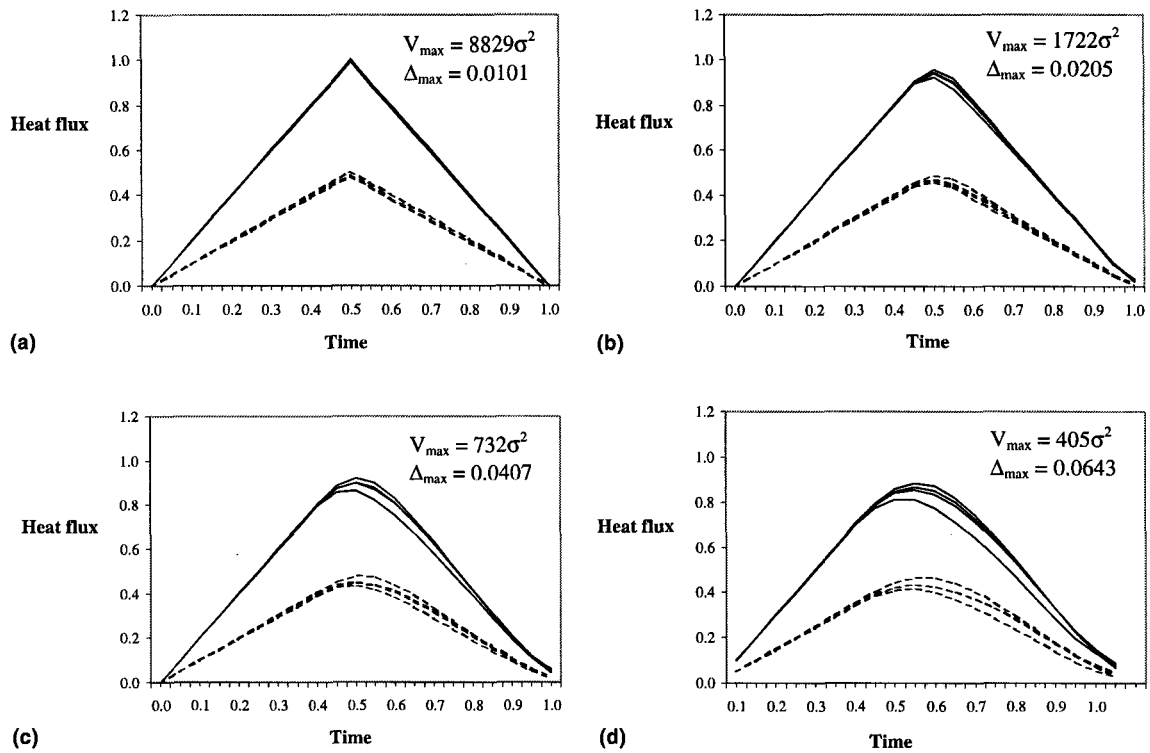

Fig. 6. Variations of heat flux components with time for (a) $r = 1$, (b) $r = 2$, (c) $r = 3$, and (d) $r = 4$. Dashed curves and solid curves represent, respectively, heat flux distribution along AB and BC. Other parameters are $x = 1/12$ and $n = 8$. Maximum variance and maximum deterministic bias are shown for each case.

the sensors. In Fig. 7, the results from four cases are compared. For each case, the number of heat flux components is six, and there are 13 sensors. The placement of sensors is illustrated in Fig. 1. It can be seen that the solution is more accurate and less sensitive to temperature measurement errors as sensors are placed closer to AB and BC. For the case where $x = 1/3$, variance is very large, and the estimated heat flux components will be very sensitive to even small statistical fluctuation in temperature measurements. It is also found that the maximum number of heat flux components that can be estimated using the inverse algorithm when sensors are placed at $x = 1/3$ is six. Increasing this number will not only increase variance but also give rise to an unstable solution, which oscillates strongly with time. Thus, there seems to be a limit to the number of heat flux compo-

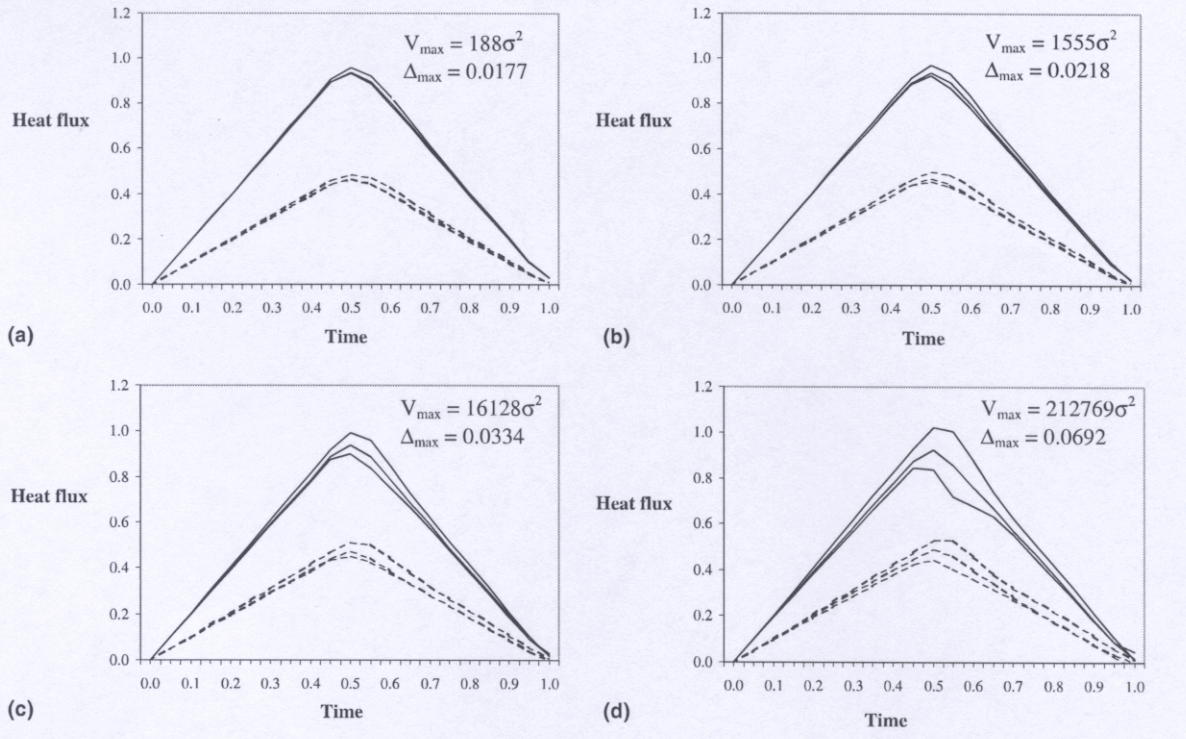

Fig. 7. Variations of heat flux components with time for (a) $x = 1/12$, (b) $x = 1/6$, (c) $x = 1/4$, and (d) $x = 1/3$. Dashed curves and solid curves represent, respectively, heat flux distribution along AB and BC. Other parameters are $n = 6$ and $r = 2$. Maximum variance and maximum deterministic bias are shown for each case.

nents that can be estimated for given number and locations of sensors.

It is interesting to compare the proposed sequential function specification algorithm with an alternative algorithm in which heat flux is assumed to be constant rather than varying linearly with time. This alternative algorithm was proposed by Beck et al. [1]. In order to use it, the present algorithm must be slightly modified. The following equations are to replace Eqs. (28)–(30):

$$B^{(0)} = \left[X^{(0)} \;\; X^{(1)} + X^{(0)} \;\; \cdots \;\; \sum_{i=0}^{r-1} X^{(r-i-1)} \right]^{\mathrm{T}} \tag{42}$$

$$B^{(j)} = \left[X^{(j)} \;\; X^{(j+1)} \;\; \cdots \;\; X^{(j+r-1)} \right]^{\mathrm{T}} \quad (j = 1, 2, \ldots, k-1). \tag{43}$$

Fig. 8 shows solutions obtained by the alternative algorithm. It should be compared with Fig. 7(a). The proposed algorithm appears to yield a better solution because it gives lower variance and lower deterministic bias. In a previous work by Chantasiriwan [11], it was shown, for the one-dimensional IHCP, that the algorithm using the assumption of linearly varying heat flux was superior to the algorithm using the assumption of constant heat flux. The present work confirms previous results in the case of the multidimensional IHCP.

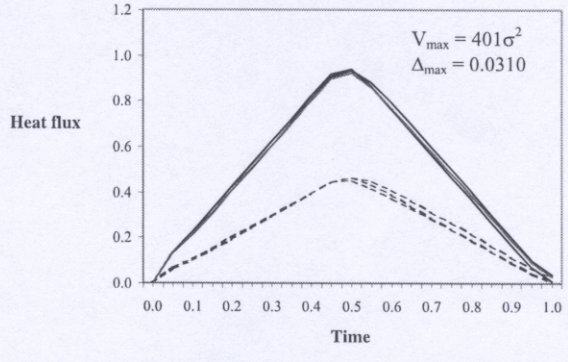

Fig. 8. Estimated heat flux for $x = 1/12$, $n = 6$, and $r = 2$ obtained by using the alternative algorithm.

8. Conclusion

The multidimensional IHCP may be solved numerically by the sequential function specification method using the assumption that heat flux varies linearly with time. The method of discretization used should be the boundary element method because it is able to deal with arbitrary geometry and requires only boundary mesh generation. The quality of the solution depends on variance, which indicates how sensitive the solution is to

errors in temperature measurements, and deterministic bias, which indicates the difference between the estimated heat flux and the actual heat flux. By decreasing the number of estimated heat flux components, increasing the future-time parameter, or placing sensors closer to the boundary of unknown heat flux, the variance of the solution will be reduced. However, there is usually a trade-off between variance and deterministic bias. Decreasing the number of heat flux components will lead to the inability to reproduced actual heat flux that varies strongly in space, and increasing the future-time parameter will result in a less accurate solution.

Acknowledgements

The author would like to acknowledge the financial support from the Thailand Research Fund.

References

[1] J.V. Beck, B. Blackwell, St. Clair Jr., Inverse Heat Conduction: Ill-posed Problems, Wiley/Interscience, New York, 1985.

[2] D. Lesnic, L. Elliott, D.B. Ingham, Application of the boundary element method to inverse heat conduction problems, International Journal of Heat and Mass Transfer 39 (1996) 1503–1517.

[3] J. Blum, W. Marquardt, An optimal solution to inverse heat conduction problems based on frequency–domain interpretation and observers, Numerical Heat Transfer, Part B 32 (1997) 453–478.

[4] M. Sassi, M. Raynaud, New space-marching method for solving inverse boundary problems, Numerical Heat Transfer, Part B 34 (1998) 21–38.

[5] L. Elden, Solving an inverse heat conduction problem by a method of lines, Journal of Heat Transfer 119 (1997) 406–412.

[6] A.M. Osman, K.J. Dowding, J.V. Beck, Numerical solution of the general two-dimensional inverse heat conduction problem (IHCP), Journal of Heat Transfer 119 (1997) 38–45.

[7] N. Al-Khalidy, A general space marching algorithm for the solution of two-dimensional boundary inverse heat conduction problems, Numerical Heat Transfer, Part B 34 (1998) 339–360.

[8] J. Taler, W. Zima, Solution of inverse heat conduction problems using control volume approach, International Journal of Heat and Mass Transfer 42 (1999) 1123–1140.

[9] N.M. Al-Najem, A.M. Osman, M.M. El-Refaee, K.M. Khanafer, Two dimensional steady-state inverse heat conduction problems, International Communications in Heat and Mass Transfer 25 (1998) 541–550.

[10] T.J. Martin, G.S. Dulikravich, Inverse determination of steady heat convection coefficient distributions, Journal of Heat Transfer 120 (1998) 328–334.

[11] S. Chantasiriwan, Comparison of three sequential function specification algorithms for the inverse heat conduction problem, International Communications in Heat and Mass Transfer 26 (1999) 115–124.

[12] P.K. Banerjee, R. Butterfield, in: Boundary Element Methods in Engineering Science, McGraw-Hill, London, 1981, pp. 216–241.